Journal of Computer and Communications, 2016, 4, 88-94
Published Online March 2016 in SciRes. http://www.scirp.org/journal/jcc
http://dx.doi.org/10.4236/jcc.2016.43014

Channel Error Estimation Methods Comparison under Different Conditions for Multichannel HRWS SAR Systems

Tingting Jin[1,2], Xiaolan Qiu[1], Donghui Hu[1], Chibiao Ding[1]

[1]Institute of Electronics, Chinese Academy of Sciences, Beijing 100190, China
[2]University of Chinese Academy of Sciences, Beijing, 100190, China
Email: 741845975@qq.com

Received 2 November 2015; accepted 26 February 2016; published 2 March 2016

Abstract

Multichannel synthetic aperture radar (SAR) in azimuth can resolve the contradiction between high resolution and wide swath faced with traditional SAR imaging. However, channel errors will degrade the performance of imaging. This paper compares the performances of four channel error estimation algorithms under different clutter distributions and SNR conditions. Further, explanations are given for performance differences of the four algorithms, which provide evidence for method selection in engineering applications.

Keywords

Synthetic Aperture Radar (SAR), High Resolution and Wide Swath (HRWS), Multi-Channel in Azimuth, Channel Error Estimation

1. Introduction

Conventional SAR system suffers from the limitation of achieving high resolution and wide swath (HRWS) simultaneously [1]-[10]. Multichannel in azimuth HRWS SAR, combined with digital beam forming (DBF) technique [2] [7], can effectively deal with this problem. Channel mismatch, caused by central electronic equipment, antenna array and satellite platform, and so on, will seriously affect the image quality in multichannel SAR systems. So channel error estimation and compensation becomes very crucial [2].

This paper mainly deals with the problem of channel errors in multi-channel HRWS SAR systems. In recent years many algorithms have been put forward to estimate the channel errors. The four main methods are time-domain correlation method (TDCM) [3], orthogonal subspace method (OSM) [4], signal subspace comparison method (SSCM) [5] [6] and antenna pattern method (APM) [5] [6]. Some simple comparisons of these methods have also been done [5] [6]. However, the performances of the estimation methods have only been compared under the Gaussian clutter scenes without theoretical analysis. In this paper, comprehensive comparison is done under different SNR conditions and different clutter distributions. In addition, theoretical analysis is given to explain the differences. The results and analysis will provide evidence for method selection in real engineering

How to cite this paper: Jin, T.T., Qiu, X.L., Hu, D.H. and Ding, C.B. (2016) Channel Error Estimation Methods Comparison under Different Conditions for Multichannel HRWS SAR Systems. *Journal of Computer and Communications*, **4**, 88-94.
http://dx.doi.org/10.4236/jcc.2016.43014

applications.

2. Echo Model

The geometric model of an actual multi-channel SAR system is shown in **Figure 1**. Δx_m, Δy_m and Δz_m denote the antenna position measurement error along X, Y, and Z axis, respectively.

Taking the channel errors caused by several factors into account [2], the total magnitude error and phase error of the *m*th channel can be denoted as $\Gamma_{c,m}$ and ζ_m. Echo of the *m*th channel can be expressed as:

$$S_{c,m}(f_r,\eta)=\iint \Gamma_{c,\mathrm{m}}\exp(\mathrm{j}\zeta_m)\sigma(x,y)H(f_r)g\left(\eta-\frac{x-x_m-\Delta x_m}{v_s}\right), \cdot\exp(\frac{-j4\pi(f_c+f_r)R_m(x,y,\eta)}{c})\mathrm{d}x\mathrm{d}y \tag{1}$$

where

$$R_m(x,y,\eta)=\sqrt{(x-x_m-\Delta x_m-v_s\eta)^2+y^2+h_z^2}\,. \tag{2}$$

3. Error Estimation Methods

Since channel magnitude errors can be estimated and compensated by simple channel balancing [5], this paper mainly concerns channel phase error estimation methods.

3.1. Time-Domain Correlation Method (TDCM)

The TDCM is presented in [3]. This estimation algorithm is operated in time-domain. Firstly, the echoes received by adjacent channels are multiplied in time-domain to get the interferometry

$$\Delta s_m(\tau,\eta)=s_m(\tau,\eta)s_{m-1}^*(\tau,\eta)=s_m\left(\tau,\eta+\frac{x_m}{v_s}\right)s_{m-1}^*\left(\tau,\eta+\frac{x_{m-1}}{v_s}\right)e^{j(\zeta_m-\zeta_{m-1})}, \tag{3}$$

where $s_m(\tau,\eta)$ is the echo of the *m*th channel, and η denoted the slow-time.

From the principle of the average cross correlation method in the baseband Doppler centroid estimation, there is

$$\angle\left\{E\left[\Delta s_m(\tau,\eta)\right]\right\}=\angle\left\{e^{j2\pi f_{dc}(x_m-x_{m-1})/v_s}e^{j(\zeta_m-\zeta_{m-1})}\right\}\Rightarrow\zeta_m-\zeta_{m-1}=\angle\left\{E\left[\Delta s_m(\tau,\eta)\right]e^{-j2\pi f_{dc}(x_m-x_{m-1})/v_s}\right\}, \tag{4}$$

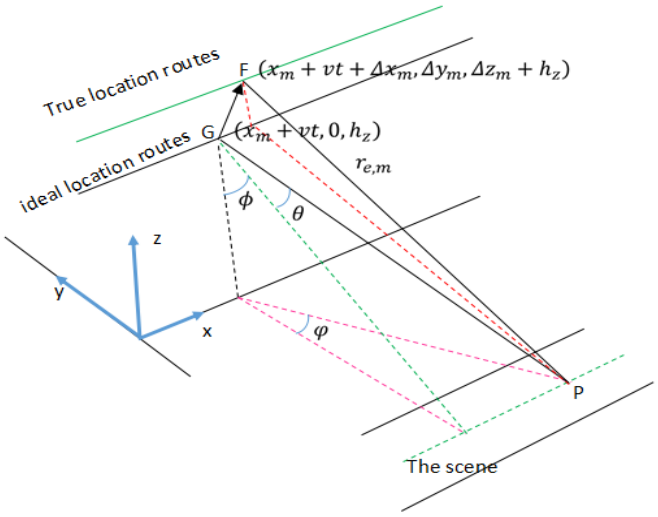

Figure 1. Geomentry of a multichannel SAR system.

where f_{dc} is the Doppler centroid.

Assume that the first channel is the reference channel, phase error of the *m*th channel is

$$\zeta_m = \sum_{i=1}^{m} (\zeta_i - \zeta_{i-1}). \tag{5}$$

3.2. Orthogonal Subspace Method (OSM)

The OSM is presented in [4]. This algorithm utilizes the orthogonality between the signal subspace and noise subspaces after eigenvalue decomposition, which is processed in Doppler domain.

Channel phase errors are estimated by minimize the cost function:

$$J = \arg\min_{G_a} \sum_{i=-I}^{I} (G_a \cdot \mathrm{a}_i)^H S_n S_n^H (G_a \cdot \mathrm{a}_i), \tag{6}$$

where a_i is the array steering vector, and G_a is a square matrix whose diagonal elements are phase errors in exponential form. S_n corresponds to the noise subspace, whose column vectors are noise eigenvectors.

Let the first channel be the reference channel, and denote $w = [1, 0..., 0]^T$. The estimation of phase errors can be expressed as

$$\hat{G}_a = diag\left(\frac{\Omega_1^{-1} w}{w^T \Omega_1^{-1} w} \right), \tag{7}$$

$$\text{where.} \quad \Omega_1 = \sum_{i=-I}^{I} \left(diag(\mathrm{a}_i) \right)^H S_n S_n^H diag(\mathrm{a}_i) \tag{8}$$

3.3. Signal Subspace Comparison Method (SSCM)

The SSCM is expressed in [5]. This algorithm makes use of the fact that the space spanned by the signal subspace eigenvectors is the same as the space spanned by the array steering vector

$$span\{G_a \cdot A(f_a)\} = span\{u_1, \cdots, u_N\}. \tag{9}$$

$$\text{Let} \quad U = \{\mathrm{u}_1, \mathrm{u}_2, ... \mathrm{u}_N\} \tag{10}$$

According to the uniqueness of orthogonal projection operator, we can get

$$U\left(U^H U\right)^{-1} U^H = GA\left(A^H G^H GA\right)^{-1} A^H G^H. \tag{11}$$

Let $V = UU^H$, $Q = G\left(G^H G\right)^{-1} G^H$, then

$$V_{m1} - G_{mm} Q_{m1} G^*_{11} = V_{m1} - Q_{m1} e^{j(\zeta_m - \zeta_1)} = 0 \Rightarrow \zeta_m - \zeta_1 = \angle \frac{V_{m1}}{Q_{m1}}, \quad \mathrm{m} = 1, ..., \mathrm{M}. \tag{12}$$

3.4. Antenna Pattern Method (APM)

The APM is expressed in [6]. This algorithm estimates the channel phase errors by combining with the antenna pattern.

Let $B = G_a \cdot A, \mathrm{C} = \mathrm{B}^H$. Ignoring the effect of noise, from the first column of the correlation matrix, there is

$$r_{m1} = \sum_{n=1}^{N} b_{mn} \sigma_{s,n}^2 c_{n1} = \sum_{n=1}^{N} b_{mn} \sigma_{s,n}^2 b_{1n}^* = \exp\left[j(\zeta_m - \zeta_1) \right] \sum_{n=1}^{N} \sigma_{s,n}^2 c_{n1} \exp\left[j2\pi \frac{\Delta x_m}{2v} \left(f_a + (-L + n - 1) \right) \bullet f_p \right]. \tag{13}$$

Then the relative phase error of the *m*th channel can be expressed by

$$\zeta_m - \zeta_1 = \angle \left(\frac{r_{m1}}{\sum_{n=1}^{N} \sigma_{s,n}^2 \exp\left[j2\pi \frac{\Delta x_m}{2v} \left(f_a + (-L + n - 1) \right) \bullet f_p \right]} \right). \tag{14}$$

4. Performance Comparison and Analysis

In this section, experiment is done to compare the performance of the above mentioned four algorithms. The parameters are listed in **Table 1**, where M is the number of channels, L_a is the antenna size in azimuth, λ is the wavelength, $\mathrm{PRF_M}$ is the pulse repetition frequency, and v_s is the velocity of platform. **Figure 2** shows a brief illustration of transmitting and receiving of the SAR system.

To compare the four methods discussed above, we use two indexes: estimation deviation and the maximum azimuth ambiguity-to-signal ratio ($\mathrm{AASR_{MAX}}$). Estimation deviation means the bias between the real phase error and the estimated phase error. $\mathrm{AASR_K}$ is the ratio of power of kth (k = 1 - 8) ambiguity component to power of the ambiguity free signal after phase error estimation and compensation [3], *i.e*.

$$AASR_K = 10 \cdot \log \frac{P_K}{S}. \tag{15}$$

Besides, $\mathrm{AASR_{MAX}}$ is the maximum of $\mathrm{AASR_K}$ (k = 1 - 8).

4.1. Estimation Performance Versus SNR

In this section, clutters are assumed to be Gaussian distribution, and SNR varies from 0 dB to 20 dB. The estimation deviations of eight channels are illustrated in **Figure 3**. The maximum estimation deviations and $\mathrm{AASR_{MAX}}$ are listed in **Table 2** for different SNR.

4.2. Performance Comparison under Different Clutter Distributions

In engineering application, clutter scenario does not obeyideal Gaussian distribution. Log-normal distribution, Weibull distribution and K-distribution are mainly considered as sea clutter model when HRWS SAR detects the seasurface.

This section mainly compares the performance of the four algorithms when clutter obeys Log-normal distribution, Weibull distribution and K-distribution, respectively. The estimation deviations of eight channels under SNR = 0 dB are illustrated in **Figure 4**. The maximum estimation deviations and $\mathrm{AASR_{MAX}}$ for different clutter distributions and different SNR are listed in **Table 3** and **Table 4**, respectively.

4.3. Analysis of the Results

Without eigenvalue decomposition and matrix inversion, the computational load of TDCM is the lowest. However, TDCM works worse than the other three algorithms under all simulated clutter distributions and SNR, for the deviation is cumulative when the phase error accumulates.

APM also does not need eigenvalue decomposition and matrix inversion, which is characterized by light computational load. But this method only applies to uniform distribution scenes. When the clutter obeys Weibull distribution and K-distribution, it works worse than OSM and SSCM under low SNR conditions (0 - 10 dB). While under high SNR conditions (>10 dB), the differences of APM, OSM, and SSCM are very small. The frequency spectrums of Weibull distribution and K-distribution are not quite homogeneous, so the performance of APM deteriorates when the noise is relatively large. For Gaussian distribution and Log-normal distribution clutters, the scenarios are homogeneous, so APM works as well as OSM and SSCM.

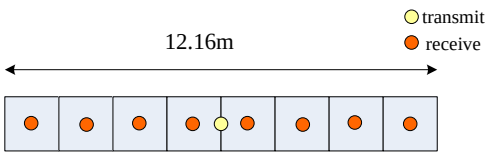

Figure 2. Illustration of transmitting and receiving of eight-channel SAR system.

Table 1. Parameters of multi-channel SAR system.

M	L_a (m)	λ (m)	$\mathrm{PRF_M}$ (Hz)	v_s (m/s)
8	12.16	0.054	1.054×10^4	7.587×10^3

Table 2. Maximum estimation deviations and $AASR_{MAX}$ for four algorithms.

Performance indicator	SNR (dB)	TDCM	OSM	SSCM	APM
Maximum estimation deviations (degree)	0	−4.5426	1.3959	1.3959	−2.0650
	5	−4.2495	0.8181	0.8181	−0.9042
	10	−4.0334	0.4654	0.4654	0.4852
	20	−3.2007	−0.2280	−0.2280	−0.2215
AASRMAX (dB)	0	−38.0153	−42.6855	−42.6855	−39.9564
	5	−37.3947	−45.9853	−46.3163	−44.2362
	10	−38.2960	−49.5419	−49.5419	−50.0598
	20	−39.4288	−51.4076	−51.4076	−51.3883

Table 3. Maximum estimation deviations for four algorithms under three clutter distributions.

Clutter Distribution	SNR(dB)	TDCM	OSM	SSCM	APM
Log-normal distribution	0	−1.8387	−1.7378	−1.7378	−1.7966
	10	−1.1058	−0.5793	−0.5793	−0.5430
	20	−0.8439	−0.2104	−0.2104	−0.1943
Weibull distribution	0	−2.2719	2.9642	2.9642	4.3430
	10	3.3355	0.8791	0.8791	1.0050
	20	4.2251	0.2599	0.2599	0.2721
K-distribution	0	5.6282	−2.1395	−2.1395	−3.5778
	10	4.7262	−0.7711	−0.7711	−0.8575
	20	3.9462	−0.2767	−0.2767	−0.2820

Table 4. $AASR_{MAX}$ for four algorithms under three clutter distributions.

Clutter Distribution	Before error compensation	SNR (dB)	TDCM	OSM	SSCM	APM
Log-normal distribution	−25.1927	0	−43.2373	−46.0874	−46.0874	−42.6242
		10	−45.7383	−50.1350	−50.1350	−50.4650
		20	−46.9298	−51.5807	−51.5807	−51.4993
Weibull distribution	−25.1927	0	−35.1346	−38.9284	−38.9284	−33.5966
		10	−39.1445	−47.2660	−47.1231	−46.1919
		20	−40.1673	−51.5414	−51.5371	−51.7242
K-distribution	−25.1927	0	−36.2404	−39.2750	−40.0067	−34.1553
		10	−40.6513	−46.1806	−46.6014	−42.3101
		20	−40.3331	−50.9115	−50.5628	−49.9990

The OSM and SSCM use the signal subspace and noise subspaces after eigenvalue decomposition of the correlation matrix, respectively. Assuming L Doppler bins are used to estimate the phase errors, the computational load of OSM and SSCM are 2 LM^3 and $LM^3 + M^3$, respectively. Their performances are best under all simulated clutter distribution and SNR conditions.

In application, when the scenes are homogeneous, such as agricultural and natural areas, APM can be chosen to estimate the channel phase errors for its accuracy and light computational load. In contrast, for heterogeneous scenes such as urban or sea surfaces, OSM and SSCM are suitable for phase error estimation.

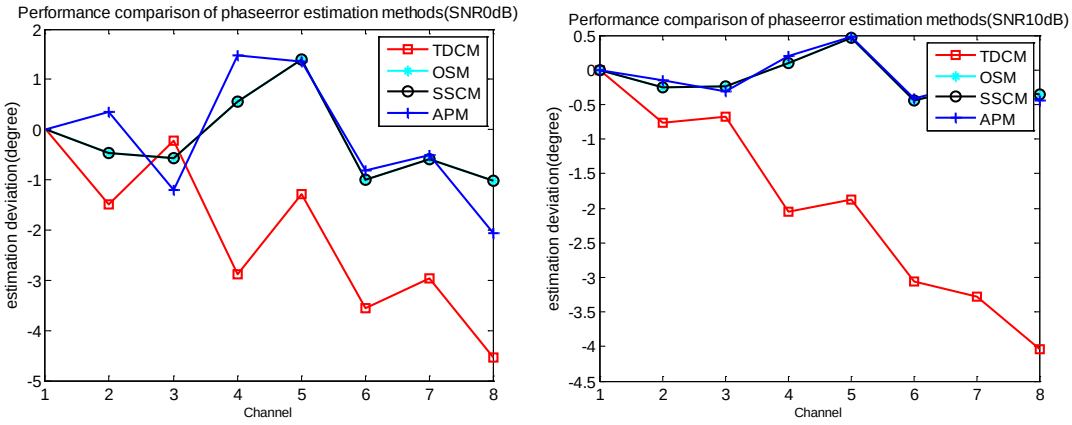

(a) (b)

Figure 3. Estimation deviations of eight channels versus SNR for the time-domain correlation method (dashed red), the orthogonal subspace method (dashed green), the signal subspace comparison method (dashed black), the antenna pattern method (dashed blue). SNR = 0 dB corresponds to **Figure 3(a)**, and SNR = 10 dB corresponds to **Figure 3(b)**.

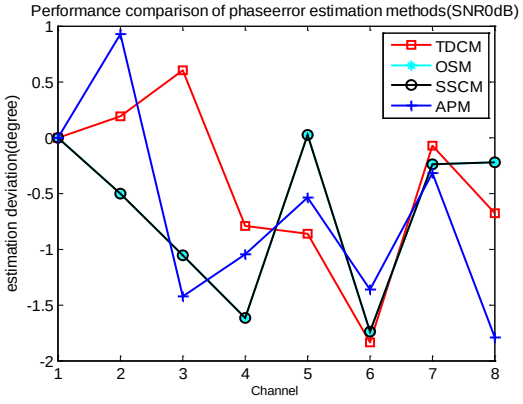

(a)

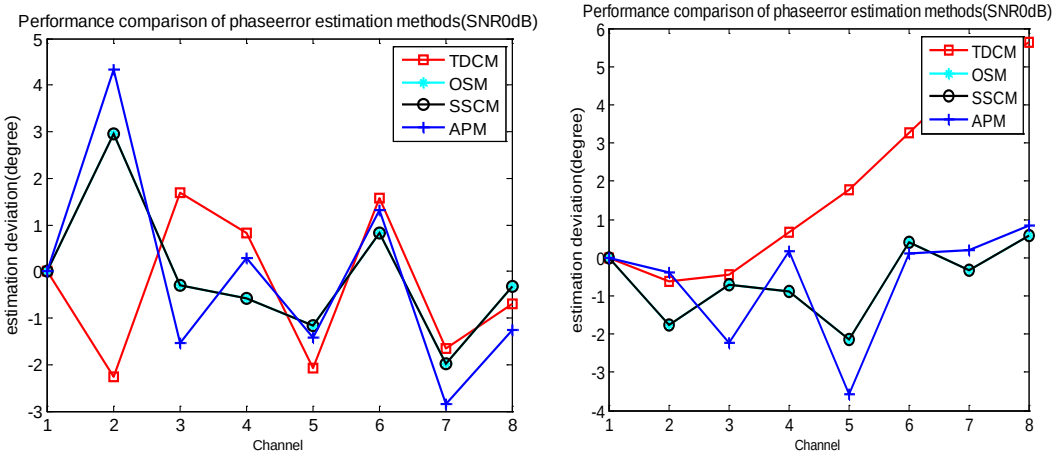

(b) (c)

Figure 4. Estimation deviations of eight channels under SNR = 0 dB. Log-normal distribution clutter corresponds to **Figure 4(a)**, Weibull distribution clutter corresponds to **Figure 4(b)**, and K-distribution clutter corresponds to **Figure 4(c)**.

5. Conclusion

In this paper, four channel error estimation methods for multichannel HRWS SAR system are compared under different SNR conditions and clutter distributions. From the simulation results, we can conclude that the estimation deviations are not relevant to real phase error distribution, and only relate to SNR and the clutter distribution. In addition, the performance of time-domain correlation method is poorer than the other three methods. For Doppler-domain methods, the APM works as well as the OSM and SSCM for homogeneous clutter scenes, but worse than OSM and SSCM for heterogeneous surfaces. OSM and SSCM work best for all clutter scenes.

References

[1] Gebert, N., Krieger, G. and Moreira, A. (2009) Digital Beamforming on Receive: Techniques and Optimization Strategies for High-Resolution Wide-Swath SAR Imaging. *IEEE Transactions on Geoscience and Remote Sensing*, **45**, 564-592.

[2] Zhang, S.X., Xing, M.D., Xia, X.G., Liu, Y.Y., Guo, R. and Bao, Z. (2013) A Robust Channel-Calibration Algorithm for Multi-Channel in Azimuth HRWS SAR Imaging Based on Local Maximum-Likelihood Weighted Minimum Entropy. *IEEE Transactions on Image Processing*, **22**, 5294-5305. http://dx.doi.org/10.1109/TIP.2013.2274387

[3] Liu, Y.Y., Li, Z.F., Suo, Z.Y. and Bao, Z. (2013) A Novel Channel Phase Bias Estimation Method for Spaceborne Along-Track Multi-Channel HRWS SAR in Time-Domain. IET International Radar Conference, China.

[4] Liu, Y.Y., Li, Z.F., Suo, Z.Y. and Bao, Z. (2010) Adaptive Two-Step Calibration for High Resolution and Wide-Swath SAR Imaging. *IET Radar Sonar Navigation*, **4**, 548-559.

[5] Yang, T.L., Li, Z.F., Liu, Y.Y. and Bao, Z. (2013) Channel Error Estimation Methods for Multichannel SAR Systems in Azimuth. *IEEE International Geoscience and Remote Sensing letters*, **10**, 548-552. http://dx.doi.org/10.1109/LGRS.2012.2212873

[6] Yang, T.L., Li, Z.F., Liu, Y.Y., Suo, Z.Y. and Bao, Z. (2013) Channel Error Estimation Methods for Multi-Channel HRWS SAR Systems. *IEEE International Geoscience and Remote Sensing Symposium*, Australia, 4507-4510.

[7] Kim, J.-H., Younis, M., Prats-Iraola, P., Gabele, M. and Krieger, G. (2013) First Spaceborne Demonstration of Digital Beamforming for Azimuth Ambiguity Suppression. *IEEE Transactions on Image Processing*, **55**, 579-590. http://dx.doi.org/10.1109/tgrs.2012.2201947

[8] Gebert, N., de Almeida, F.Q. and Krieger, G. (2011) Airborne Demonstration of Multichannel SAR Imaging. *IEEE Geoscience and Remote Sensing Letters*, **8**, 963-967. http://dx.doi.org/10.1109/LGRS.2011.2144563

[9] Zhang, S.X., Xing, M.D., Xia, X.G., Zhang, L., Guo, R., Liao, Y. and Bao, Z. (2014) Multichannel HRWS SAR Imaging Based on Range-Variant Channel Calibration and Multi-Doppler-Direction Restriction Ambiguity Suppression. *IEEE Transactions on Geoscience and Remote Sensing*, **52**, 4306-4327. http://dx.doi.org/10.1109/TGRS.2013.2281329

[10] Li, Z.F., Bao, Z., Wang, H.Y. and Liao, G.S. (2004) Performance Improvement for Constellation SAR Using Signal Processing Techniques. *IEEE International Geoscience and Remote Sensing Letters*, **1**, 436-452.